

CONTROL OF LASER RADIATION PARAMETERS

PACS numbers: 42.55.Lt; 42.60.Jf; 42.60.Cf
DOI: 10.1070/QE2001v031n09ABEH002053

Space – time structure of radiation from a high-power fast-flow CO_2 laser

V A Gurashvili, A M Zotov, P V Korolenko, A P Napartovich, S P Pavlov, A V Rodin, N E Sarkarov

***Abstract*. The space – time structure of radiation from an industrial electric-discharge, flowing CO_2 laser is studied experimentally. For the optimal design of the optical and gas-dynamic sections, a total suppression of high-frequency radiation fluctuations and a lowering of the amplitude of low-frequency fluctuations down to 6 % – 10 % were observed with increasing output power. At the same time, the intensity distribution in the near-field diffraction zone was complicated and unstable. 'Hot' spots and screw wave-front dislocations were observed in the laser-beam cross section. Numerical simulations showed that the properties of the near-field radiation structure are determined by random caustics and phase singularities formed due to the diffraction transformation of the initial wave-front perturbations.**

Keywords: *industrial laser, laser-radiation quality, wave-front dislocations.*

1. Introduction

There exists a number of physical factors which complicate the space – time structure of radiation of fast-flow industrial CO_2 lasers. The high peak intensities inherent in these lasers enhance optical inhomogeneities of the active medium, lead to thermal deformations of the reflecting surfaces of resonator mirrors, cause the nonlinear self-action in the active medium, and initiate the multimode oscillation regime [1, 2]. An important part in the instability development is played by self-modulation processes. They typically occur in transverse-flow lasers in which an unstable resonator and a scheme with separate pumping and oscillation are used. The power self-oscillations with a period close to the time of flight through the resonator result in the power modulation degree up to 100 % [3, 4].

The flow-velocity inhomogeneities of the active medium may result in the stabilisation of the oscillation regime [5], however, they enhance the phase inhomogeneities of the medium [6]. Because the complicated factors that perturb the radiation structure have not been adequately investigated, their combined effect is frequently estimated by specifying the statistical parameters of the phase distribution in the output laser beam with a subsequent determination of the far-field beam characteristics [7]. This is accomplished by separating the 'regular' component in the initial phase distribution, which determines the average surface of the wave front.

The properties of the near-field zone of laser beams, which can be quite long for wide-aperture lasers, have received far less attention. In this paper, we analyse the perturbations of the radiation field of a 10.6-μm electric-discharge flowing CO_2 laser and estimate the effect of self-modulation processes and small-scale wave-front distortions on the space–time near-field radiation structure.

2. Laser characteristics and measuring technique

The design of the laser under study was described in detail earlier [8, 9]. The active medium in the resonator cavity was produced by admixing the CO_2 gas component to the binary N – He mixture vibrationally pre-excited in a gas-discharge chamber. The chamber design furnished an energy input up to 400 J g^{-1}. The circulation rate of the active medium was varied in the 100 – 150 m s^{-1} range. The pumping regime, the gas composition, and the characteristics of the optical resonator were varied in experiments. The modulation depth of the energy input in the discharge in the working regimes was no greater than 5 % and the instability of gas-dynamic parameters did not exceed 3 %.

To extract the energy from the laser active medium, different unstable resonator configurations with the magnification $M = 1.12 - 2.2$ were used. The radiation passes through the active laser medium once or twice, depending on the resonator design. In a double-pass unstable resonator, corner reflectors consisting of two or three plane mirrors were used. The application of these reflectors provides not only efficient illumination of the active medium, but also levels off the intensity distribution in the transverse beam section owing to the rotation of the field in the resonator cavity. The cross section of the radiation escaping from the resonator could be shaped into a rectangular, a square, or a circle, with their central part being screened by the output mirror. In the majority of experiments, a double-pass resonator configuration with corner reflectors shown in Fig. 1a was employed. Fig. 1b shows the characteristic beam shape at the laser output. The outer aperture of the beam was varied from 50 to 70 mm.

V A Gurashvili, A P Napartovich, S P Pavlov, A V Rodin, N E Sarkarov Troitsk Institute of Innovation and Fusion Research, 142092 Troitsk, Moscow oblast, Russia;
A M Zotov, P V Korolenko M V Lomonosov Moscow State University, Vorob'evy gory, 119899 Moscow, Russia;
e-mail: korolenko@optics.npi.msu.su

Received 8 February 2001
Kvantovaya Elektronika **31** (9) 821 – 824 (2001)
Translated by E N Ragozin

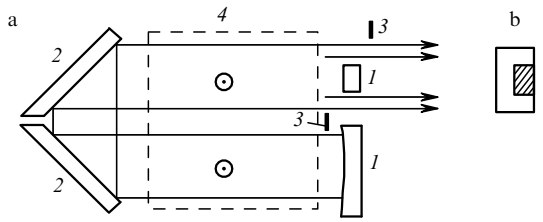

Figure 1. Schematic diagram of the resonator (a) and beam shape at the laser output (b): (*1*) spherical mirrors; (*2*) mirrors of the corner reflector; (*3*) apertures; (*4*) active medium. The dashed fragment in Fig. 1b corresponds to the region screened by the output mirror; ⊙ indicates the flow direction.

Fluctuations of power and intensity distribution in the cross section of the output beam were measured in an attenuated laser beam. The laser beam intensity was attenuated using ruled diffraction gratings made on glass substrates, diffraction couplers on a basis of mirrors with a regular perforation structure, and also couplers made as narrow strips of spherical mirrors. KCl or ZnSe optical wedges were additionally used when the attenuation was not sufficient.

FSG-223 photoresistors or HgCdTe IR detectors were employed as photodetectors. The radiation was recorded directly or via an integrating sphere, depending on the power of the attenuated laser beam. Small spherical mirrors 5–10 mm in diameter were mounted to measure the intensity distribution in the cross section of the beam. By scanning the output beam aperture with the help of these mirrors we could record the intensity distribution with a resolution of 3–7 mm in any selected beam section. The scan time of the beam aperture was $10^{-2} - 10^{-3}$ s.

3. Experimental results and their interpretation

We found that the average amplitude of the output power fluctuations in the double-pass resonator did not exceed 6 %–10 % for the resonator magnification factor $M = 1.5$. Fig. 2 shows an oscilloscope trace of the total output power typical for this magnification factor. The variation in the resonator magnification factor in the limits $M = 1.5 - 2.2$ did not result in noticeable changes in the time dependence of the output power. In this case, the power extracted from the laser active medium lowered with increasing M because the power density in the resonator was not high enough. The decrease in the magnification factor M of the unstable resonator from 1.5 to 1.1 resulted in a growth in the amplitude of power fluctuations (including those at high frequencies) corresponding to the flight time of the active medium. The reduction of the energy extraction aperture along the flow in going to the single-pass resonator also resulted in the increase in output power fluctuations. Nevertheless, even in the above unfavourable situations the power modulation depth did not exceed 20 %.

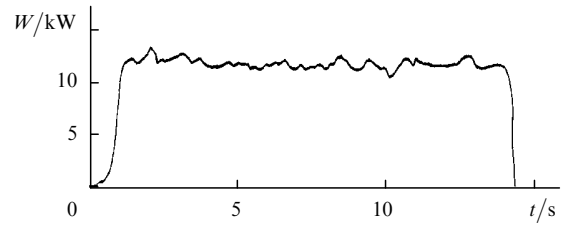

Figure 2. Fluctuations of the total output power W of the laser beam.

Note, however, that the spectrum of modulated lasing in the double-pass resonator with corner reflectors contained only low-frequency components (with frequencies below 10 Hz) for optimal magnification factors $M \approx 1.5$. This can be explained by the fact that in such a resonator there occurs an efficient averaging of the factors responsible for high-frequency power oscillations.

Unlike the total output power, the intensity in the beam cross section was highly unstable in time. In addition, its distribution over the transverse coordinates was very complicated. The diffraction fringes related to the Fresnel diffraction from resonator apertures were overlapped by randomly arranged nonstationary spots, whose intensity far exceeded the average intensity. The apertures were used to eliminate parasitic lasing channels and the high-power irradiation of the resonator elements. The coefficient of spatial modulation of the intensity distribution caused by diffraction depended on the distance between the plane of measurements and the output aperture of the resonator. In the region close to the output aperture of the resonator, the modulation depth amounted to 30 %. As the plane of measurements was removed from the output aperture, the depth of radiation intensity modulation decreased to become less than 15 % for distances exceeding 10 m.

The number of 'hot' spots in the cross section of the output beam depended on the output power. Up to six such spots were recorded for a high output power. As the output radiation power decreased, the number of spots decreased, and no more than two spots were observed for an output power of 5–6 kW. At a distance of 19 m from the output aperture, their dimensions varied in the range between 10 and 20 mm. Fig. 3 shows the characteristic intensity distributions at a fixed beam cross section measured at different moments of lasing. The intensity distributions were recorded with a time interval of 0.02 s. One can see from Fig. 3, that the distributions exhibit regions with intensities exceeding the average one by 3–7 times.

To demonstrate more clearly the recording of high-intensity regions and estimate their longitudinal dimensions, a special aerosol chamber was made, enabling a visualisation of the spatial beam fragments whose intensity exceeds a certain magnitude. Small particles of corundum suspended in air were used as the working medium in the aerosol chamber. To increase the radiation intensity and reach the threshold intensity of corundum emission, the radiation was focused with a long-focus mirror prior to passing through the aerosol chamber. This technique allowed us to investigate the evolution of the laser-beam structure from the character of corundum emission. Fig. 4 shows one of the photographs of corundum emission in the converging laser beam. The dimension of the region given in the photograph far exceeds the longitudinal dimension of the focal spot corresponding to the far-field zone. One can see from Fig. 4 that the regions with extreme intensity have the form of long narrow channels. The number and position of such channels was changing constantly during lasing.

Along with the recording of spatial radiation intensity distribution, we studied the specific features of phase distribution in the cross section of the laser beam employing a lateral shearing interferometer. An analysis of the interference patterns corresponding to a high output power (of

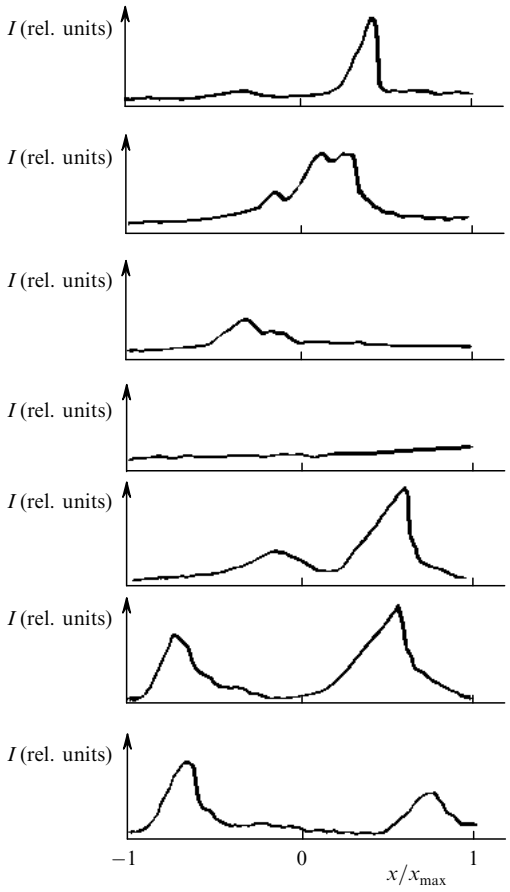

Figure 3. Intensity distributions in the laser-beam cross section (x is the transverse coordinate; from bottom to top: successive scans at 0.02-s intervals).

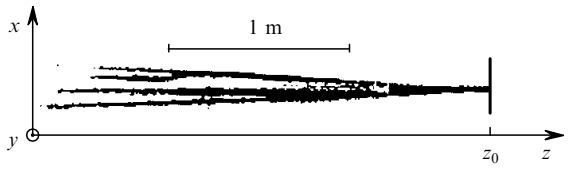

Figure 4. Emission of corundum particles in a converging laser beam (x and y are the transverse and longitudinal coordinates, respectively; z_0 is the focal plane).

the order of 10 kW) revealed the formation of screw dislocations at the wave front along with significant phase aberrations. However, on lowering the output power to 3–4 kW there occurred a drastic decrease of phase aberrations, and dislocations were no longer observable. The screw dislocations were identified from the branch points of interference fringes. Fig. 5 shows the interference pattern of a wave front with a screw dislocation. The recording of screw dislocations is consistent with previous observations [10, 11] of topological wave-front distortions in laser radiation and indicates that their formation is characteristic of the beams of a very broad class of lasers.

The mechanisms underlying the found stochastisation of amplitude-phase beam profile and the formation of 'hot' spots with a high radiation intensity can be different. One of them involves the excitation of a superposition of transverse modes in the laser resonator [2]. Another formation mechanism of complex near-field amplitude and phase distributions may be caused by transient wave-front perturbations of the output radiation. Even in the case of smooth perturbations, caustics and phase singularities may be produced in the beam due to diffraction energy redistribution when a depth of phase modulation exceeds a certain magnitude [12, 13]. The former manifest themselves as fragments of the lateral structure with extreme intensities and the latter as screw phase dislocations.

Figure 5. Interference pattern of the transverse shift of the laser beam. The frame in the pattern field indicates the position of a dislocation.

The occurrence of dislocations and caustics in a beam exhibiting in the exit plane a uniform intensity distribution and smooth random wave-front perturbations is illustrated in Fig. 6. Fig. 6 shows the intensity distributions and the lines of equal phase calculated at different distances from the exit plane. The initial distribution is uniform in intensity and its wave front is randomly modulated. The calculations were performed by the method of decomposition of the initial field into plane waves [13, 14].

In the exit plane, the intensity was uniformly distributed, while the phase distribution was so modelled that its rms deviation σ from the phase of a plane wave was equal to 0.6 rad. Such wave-front perturbations are typical for the laser under study for a high output power. One can see from Fig. 6 that the phase aberrations in the exit plane are responsible for the formation of enhanced-intensity regions of random shape and position in the lateral section and, some distance away, for the formation of screw wave-front dislocations as well (the presence of the latter is attested by the points of intersection of the lines of equal phase).

The above numerical simulation of the amplitude-phase distribution transformation showed that, as in the case of regular wave-front perturbations, the formation of screw dislocations inherently possesses a threshold [14]. As σ decreases, the density of screw dislocations lowers drastically, and their occurrence becomes unlikely for $\sigma < 0.5$, which is consistent with our experimental data. The appearance of 'hot' spots and phase singularities in the beam cross section thereby receives a simple explanation in the context of the model considered above. When it is necessary to eliminate the formation of phase singularities and local intensity zeroes associated with them, the parameters of laser oscillation should remain in the range that precludes exceeding the limiting phase perturbations. Bec-

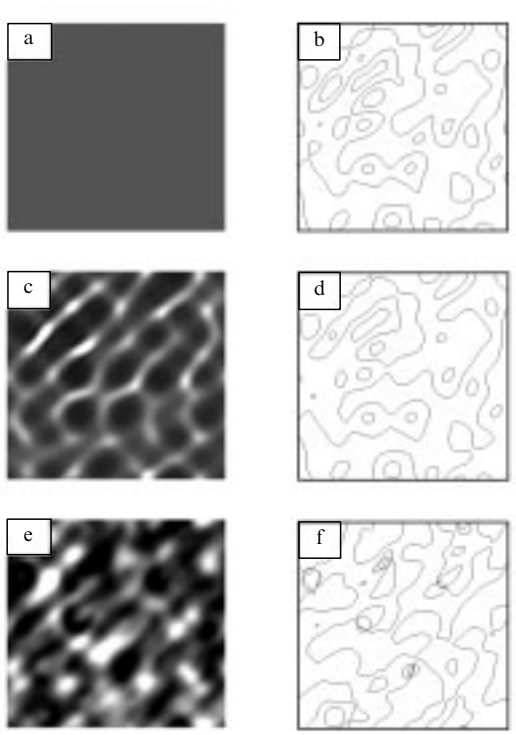

Figure 6. Calculated intensity (a, c, e) and phase (b, d, f) distributions of the radiation at distances from the exit plane $z = 0$ (a, b), $0.01A^2/2\lambda$ (c, d), and $0.5A^2/2\lambda$ (e, f) (A is the longest period of harmonics of the initial field distribution; the phase distribution in Figs b, d, and f is represented by the lines of equal phase).

ause it is difficult to determine the σ parameter directly from interferometric measurements, the determination of this parameter from the corresponding Strehl number may prove to be more convenient from the practical point of view. The above calculations showed that to a critical value $\sigma = 0.5$ there corresponds a Strehl number for a beam equal to 0.85.

4. Conclusions

Our investigation of high-power (of the order of 10 kW and above) industrial cw CO_2 lasers with a flowing active medium showed that high-frequency output-power fluctuations related to self-modulation are suppressed in optimal lasing regimes. While the total output power is stable enough, the near-field distributions of amplitude and phase in the laser beam cross section are inherently complex and unstable. The complication of radiation structure involves the formation of caustics and screw wave-front dislocations in the radiation field, which result from the diffraction transformation of initial wave-front perturbations.

Acknowledgements. This work was partly supported by the 'Physics of Quantum and Wave Processes' State Scientific and Technical Programme (Grant No. 1.61).

References

1. Golubev V S, Lebedev F V *Kvantovaya Elektron.* **12** 663 (1985) [*Sov. J. Quantum Electron.* **15** 437 (1985)]
2. Valuev V V, Naumov V G, Sarkarov N E, Svotin P A *Kvantovaya Elektron.* **25** 16 (1998) [*Quantum Electron.* **28** 14 (1998)]
3. Dreizin Yu A, Dykhne A M *Pis'ma Zh. Eksp. Teor. Fiz.* **19** 818 (1974)
4. Artamonov A V, Naumov V G *Kvantovaya Elektron.* **4** 178 (1977) [*Sov. J. Quantum Electron.* **7** 101 (1977)]
5. Likhanskii V V, Napartovich A P *Izv. Akad. Nauk SSSR Ser. Fiz.* **45** 399 (1981)
6. Artamonov A V, Napartovich A P *Kvantovaya Elektron.* **6** 1554 (1979) [*Sov. J. Quantum Electron.* **9** 913 (1979)]
7. *Moshchnye lazernye puchki v sluchaino-neodnorodnoi atmosfere* (High-Power Laser Beams in a Random Atmosphere) V A Banakh (Ed.) (Novosibirsk: Izd. SO RAN, 1998)
8. Abil'sitov G A, Velikhov E P, Golubev V S, Lebedev F V *Kvantovaya Elektron.* **8** 2517 (1981) [*Sov. J. Quantum Electron.* **11** 1535 (1981)]
9. Naumov V G, Rodin A V *Proceedings of the International Conference Lasers'94, Quebec, Canada, 1994* p. 171
10. Korolenko P V, Tikhomirov P V *Kvantovaya Elektron.* **18** 1139 (1991) [*Sov. J. Quantum Electron.* **21** 1024 (1991)]
11. Bobrov A D, Dmitriev E I, Snezhkov G Yu *Kvantovaya Elektron.* **20** 680 (1993) [*Quantum Electron.* **23** 588 (1993)]
12. Kravtsov Yu A, Orlov Yu N *Geometricheskaya optika neodnorodnykh sred* (Geometrical Optics of Inhomogeneous Media) (Moscow: Nauka, 1980)
13. Goodman J W *Introduction to Fourier Optics* (New York: McGraw-Hill, 1968)
14. Gurashvili V A, Zotov A M, Korolenko P V, Sarkarov N E *Kvantovaya Elektron.* **30** 803 (2000) [*Quantum Electron.* **30** 803 (2000)]